Entropy Generation during Cellular Magnetoconvection

Md. Abdul Rawoof Sayeed, Mohammed Majid Ali

***Abstract*—The entropy generated during the laminar natural convection of fluid under the effect of an external magnetic field is studied in this paper. The numerical simulation for total entropy generation has been carried out for nonlinear magnetoconvection. The entropy generation for laminar flow in the transient state due to fluid friction, magnetic effect as well as heat and mass transfer, have been determined for stress-free boundary conditions. The entropy generation rates play an important role in the overall thermal mixing of the fluid within the cavity. An analysis of total entropy generation (S_{gen}) is carried out for increasing values of thermal buoyancy and magnetic field using local entropy maps for the Prandtl number (Pr_1 of liquid metals ranging from 0.001 to 0.03. It is found that S_{gen} is a monotonically increasing function with Ra. It is observed that the magnetic field has a diminishing effect on heat transfer in the convective system, which in turn, leads to retarding effect on total entropy generation. It is also shown that the kinetic energy of the fluid is reduced due to the application of a vertical magnetic field.**

***Index Terms*—Entropy generation, Liquid metals, Thermal convection, kinetic energy, Magnetic field.**

I. Introduction

The magnetic diffusivity of liquid metals is higher in comparison to their thermal diffusivity. The density, thermal conductivity, viscosity and specific heat are the basic properties to be considered during heat transfer for liquid metals. Liquid metals are unique among fluids because of their high thermal conductivity and consequently low Prandtl number. The experimental studies of convection in liquid metal are also made difficult by the complexity of the thermal and dynamical measurements. Convection is an important phenomenon in crystal growth from the melt under the influence magnetic field. Thus experiments involving liquid metals are of great value in assessing the effects of high electrical and thermal conductivity. There are few experimental works on convective flows, made on liquid metals such as mercury or sodium [1]-[5]. In a horizontal layer of liquid metal, thermal convection flow is inhibited according to the magnitude of an external magnetic field. Saunders [6] was the first to perform the measurements of natural convection in liquid metal, with a uniform heat flux surface condition, using a vertical plate in mercury. The Experimental results of Saunders and his analysis were in agreement to a fair degree. Fumizawa [7] studied experimentally the effect of the magnetic field upon laminar natural convection of liquid metals using Mercury and NaK as working liquids. He imposed the magnetic field in parallel and perpendicular to the direction of gravity to the uniformly heated vertical plate. It was seen that the velocity in the fluid decreased with the increase in the magnetic field, and the temperature distribution approached the solution for pure heat conduction. He also found that the magnetic fields effects decreased the rate of heat transfer from the wall. The effects of an externally applied magnetic force on heat transfer, fluid flow and entropy generation of liquid gallium and air were analyzed in the rectangular cavity by El Jery et al [8]. Their results showed that entropy generation and heat transfer rate are reduced inside the rectangular cavity by increasing the applied magnetic field.

During the past three decades, entropy generation analysis has become a powerful tool to optimize various complicated systems. Entropy generation is a common phenomenon related to thermodynamics irreversibility, in all types of heat transfer processes. The entropy generation is responsible for various sources of irreversibility, such as characteristics of convective heat transfer, heat transfer across a finite temperature gradient, viscous dissipation effect, magnetic field effect, etc. For instance, multiple studies predicted the irreversibility phenomenon within confined cavities. The entropy generation has great importance in many engineering fields such as cooling of nuclear reactors, heat exchangers, geophysical fluid dynamics, energy storage systems, MHD power generators, cooling of electronic devices, etc. The optimal design of thermal systems can be accomplished by reducing the entropy generation in the systems.

Bejan [9]-[10], spent much effort to determine the gap among thermodynamics, heat transfer, and fluid mechanics. He applied the second law of thermodynamics to determine the entropy generations due to heat and flow transport and consequently to minimize the entropy generation. Saravanan and Kandaswamy [11] studied the convection driven by the combined mechanism of surface tension and buoyancy in a low Prandtl number fluid in the presence of a uniform vertical magnetic field. They showed that in the presence of a vertical magnetic field the heat transfer decreases from the hot wall to the cold wall as thermal conductivity diminishes.

In this paper, numerical investigations are performed to study the effect of vertical magnetic field on Rayleigh-Benard convection for electrically conducting liquid metals using entropy generation approach. The governing equations describing the temperature, motion and magnetic fields, are solved numerically using the perturbation analysis proposed by Kuo [12]. The numerical results for total entropy generation due to fluid friction and heat transfer irreversibilities have been determined for laminar magnetoconvection using

Manuscript received April 05, 2021; revised February 21, 2022.

Md. Abdul Rawoof Sayeed is Associate Professor in Department of Mathematics, Muffakham Jah College of Engineering and Technology, Hyderabad, Telangana, India 500034 e-mail: (rfsayeed@mjcollege.ac.in).

Mohammed Majid Ali is Lecturer in Department of Mathematics, University of Technology and Applied Sciences-Ibra, Sultanate of Oman: (mmali.math81@gmail.com).

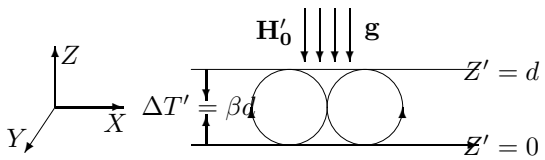

Fig. 1. Schematic diagram of the physical model.

the perturbation analysis method for stress-free boundary conditions. This numerical study is conducted for various governing parameters of magnetoconvection, whose effects on entropy generation are discussed and analyzed. The methodology adopted to study entropy generation for the physical parameters of liquid metals is similar to the numerical simulation of Rameshwar et al. [13]. The results of variation of the kinetic energy of the fluid flow under influence of applied vertical magnetic field are also studied. It is shown that the kinetic energy of the fluid is reduced by applying a vertical magnetic field. The increase in vertical magnetic field suppresses the velocity fluctuation of fluid flow in a convective system.

II. Mathematical Model

An electrically conducting fluid is considered between the two infinite horizontal planes as shown in Fig.1, with adverse temperature gradient $\Delta T'$. It is assumed that an externally applied magnetic field, $\mathbf{H}_o^{'} = H_o^{'}\hat{\mathbf{e}}_\mathbf{z}$ acts along the vertical direction. The perturbed basic governing equations in non-dimensional quantities in Boussinesq approximation, are given by

$$\nabla.\mathbf{V} = 0, \nabla.\mathbf{H} = 0, \tag{1}$$

$$\frac{1}{Pr_1}\left[\frac{\partial \mathbf{V}}{\partial t} + (\mathbf{V}.\nabla)\,\mathbf{V}\right] - Q\frac{Pr_2}{Pr_1}(\mathbf{H}.\nabla)\mathbf{H} = -\nabla\left(\frac{P_1}{Pr_1} + \frac{QPr_2}{2Pr_1}|\mathbf{H}|^2 + QH_z\right) + + Q\frac{\partial \mathbf{H}}{\partial Z} + Ra\theta\hat{\mathbf{e}}_\mathbf{z} + \nabla^2\mathbf{V}, \tag{2}$$

$$\left(\frac{\partial}{\partial t} - \nabla^2\right)\theta = w - (\mathbf{V}.\nabla)\,\theta, \tag{3}$$

$$\left(\frac{Pr_2}{Pr_1}\frac{\partial}{\partial t} - \nabla^2\right)\mathbf{H} = \nabla\times(\mathbf{V}\times\hat{\mathbf{e}}_\mathbf{z}) + + \frac{Pr_2}{Pr_1}\nabla\times(\mathbf{V}\times\mathbf{H}), \tag{4}$$

where $Ra = \alpha g\beta d^4/\kappa\nu$, $Q = \mu_m H_o^2 d^2/4\pi\rho_o\nu\eta$, $Pr_1 = \nu/\kappa$ and $Pr_2 = \nu/\eta$. In Eqs. (1)-(4), $\theta(= T - T_s)$, $\mathbf{V}$ and $\mathbf{H}$ denote the perturbed unknowns for temperature, velocity and magnetic field, respectively. The stress-free boundary conditions [14] are assumed in this study which are given by,

$$w = \frac{\partial^2 w}{\partial Z^2} = \theta = 0, H_X = H_Y = 0 \text{ and } \frac{\partial H_Z}{\partial Z} = 0 \text{ at } Z = 0, 1. \tag{5}$$

The methodology to solve the perturbed basic governing equations (1-4) along with the boundary condition (5) is similar to the numerical simulation approach adopted by Rameshwar et al. [13].

III. Entropy Generation

In the quest for effective utilization of energy resources, the process of natural convection must be proficient while transferring heat with minimum entropy generation. The present work analyzes the effects of entropy generation in magnetoconvection, which depends on the viscous effects within the fluid and the irreversible nature of heat transfer. The non-dimensional form of local entropy generation rate (S_{gen}) is given by the addition of fluid friction irreversibility (S_{FFI}) and heat transfer irreversibility (S_{HTI}).

$$S_{gen} = S_{HTI} + S_{FFI} \tag{6}$$

$$S_{HTI} = \left(\frac{\partial\theta}{\partial X}\right)^2 + \left(\frac{\partial\theta}{\partial Z}\right)^2 \tag{7}$$

$$S_{FFI} = \phi\left[2\left(\frac{\partial u}{\partial X}\right)^2 + 2\left(\frac{\partial w}{\partial Z}\right)^2 + \left(\frac{\partial u}{\partial Z} + \frac{\partial w}{\partial X}\right)^2\right] \tag{8}$$

where u and w are the non-dimensional velocities in X and Z directions, respectively, $\phi = (\mu T_0\kappa^2)/(kK(\triangle T)^2)$ is the irreversibility distribution ratio which is assumed as 10^{-4} in the present study.

IV. Result and discussion

The process of heat transfer for all real systems of engineering is studied as an irreversible process. Which is effectively associated with entropy generation. The generated entropy has an immense influence on the efficacy of the system. It abolishes the existing work and consumes the available energy of the system. It can also further add up to wastage of energy and causes a diminution in the performance of the whole system. Due to this, entropy generation becomes the principal criterion to evaluate the efficacy of all engineering machinery. The present model is described by a set of nonlinear partial differential equations involving energy equation, momentum equation and magnetic equation. The characteristics of energy distributions in the convective system are analyzed by outlaying the entropy maps of total entropy generation. From the physical point of view, the impact of several values of specified parameters on heat transfer, such as Rayleigh Number, thermal and magnetic Prandtl numbers, Chandrashekar number are explored and presented graphically in Figs. 2-6.

The total entropy generation maps for different values of Ra in the absence of a magnetic field ($Q = 0$) with $Pr_1 = 0.025$ are depicted in Figs. 2(a-c). At the onset, due to weak fluid velocities, the frictional irreversibility is low. It is observed that, at the onset of convection i.e. for $Ra \simeq Ra_o$, in Fig. (2a) the entropy maps are smooth semi-cylindrical and dense near the boundaries. The entropy

maps of higher values are located near the upper and lower boundaries. The local maximum and minimum values of S_{gen} are 0.00631 and 0, respectively. The maximum value of the total entropy generated is very small at the onset. The middle region is covered with smooth concentric cylindrical entropy maps with a minimum value of 0 at the center. This is because at the onset, the viscous force dominates and the heat transfer is mainly due to conduction. In the case of $Ra = 1.1Ra_o$, due to a higher rate of heat transfer and enhanced fluid velocities, some of the entropy maps near the lower and upper boundaries extend up to the central region, influencing nearly the half-area of the cavity as shown in Fig. 2(b). The entropy maps of the mid-region of the bottom plane and right corner of the top plane are expanded due to the higher buoyancy force. This causes the deformation of central concentric cylindrical entropy maps. The local maximum and minimum values of S_{gen} are 0.7337 and 0.0023, respectively. The maximum value of S_{gen} is increased from 0.00661 to 0.7337 as the buoyancy force increased from onset to $1.1Ra_{1o}$. High thermal gradients are concentrated near the upper and lower boundaries and hence the total entropy generated due to heat transfer irreversibility and fluid friction irreversibility is found to be high. It may be noted that the entropy maps are highly dense with high entropy gradients at lower and upper boundaries compared to the central zone with low entropy gradients. This is due to low thermal gradients in the middle region.

The entropy maps for S_{gen} are exhibited for $Ra_1 = 1.3Ra_o$ in Fig. 2(c). The entropy maps near the left bottom boundary and top right boundary extend up to the opposite side due to the enhanced rate of heat transfer and fluid velocity, as shown in Fig. 2(c). The corresponding maximum and minimum values of S_{gen} are 7.7771 and 0.0039, respectively. The maximum value of S_{gen} is increased from 0.7337 to 7.7771. Which corresponds to a higher degree of irreversibility for heat transfer and fluid flow.

In Figs. 3(a-d) the entropy maps are depicted for $Q = 1000$, $Pr_1 = 0.017$ and $Pr_2 = 0.001$ for increasing values of thermal buoyancy(Ra). The buoyancy force and magnetic effect act simultaneously along with the gravitational buoyancy and change the energy distribution are revealed by the entropy maps in Fig. 3(a-d). The entropy maps near the onset are presented in Fig. 3(a) under the influence of the magnetic field. The number of cellular patterns of entropy maps is almost doubled to that of entropy maps without the magnetic field (Fig. 2(a)), at the onset of convection in the presence of a magnetic field. The corresponding maximum and minimum values of S_{gen} are 0.0061 and 0, respectively. The magnetic susceptibility squeezes the energy distribution within the system and hence dampens the heat flow. The entropy maps for the higher value of $Rs = 1.3Ra_o$ are depicted in Fig. 3(b). The primary concentric cellular roll maps of entropy are deformed as oblique entropy maps. The local maximum and minimum values of S_{gen} are 1.3782 and 0.0324, respectively. The change in entropy maps depicts the influence of higher thermal buoyancy on energy distribution. As Ra is incremented by $Ra = 1.6 \times Ra_o$(Fig. 3(c)), convection increases due to higher buoyancy force and consequently, the rate of heat transfer is also enhanced in the system. The local maximum and minimum values of S_{gen} are 3.3225 and 0.0444, respectively. It is interesting to note that as thermal buoyancy is increased, the middle oblique entropy maps extend towards the boundary regions due to the high frictional irreversibility of the middle region of the cavity. The entropy generation due to fluid friction is confined to a small regime near the boundaries and at the central upper and lower regions.

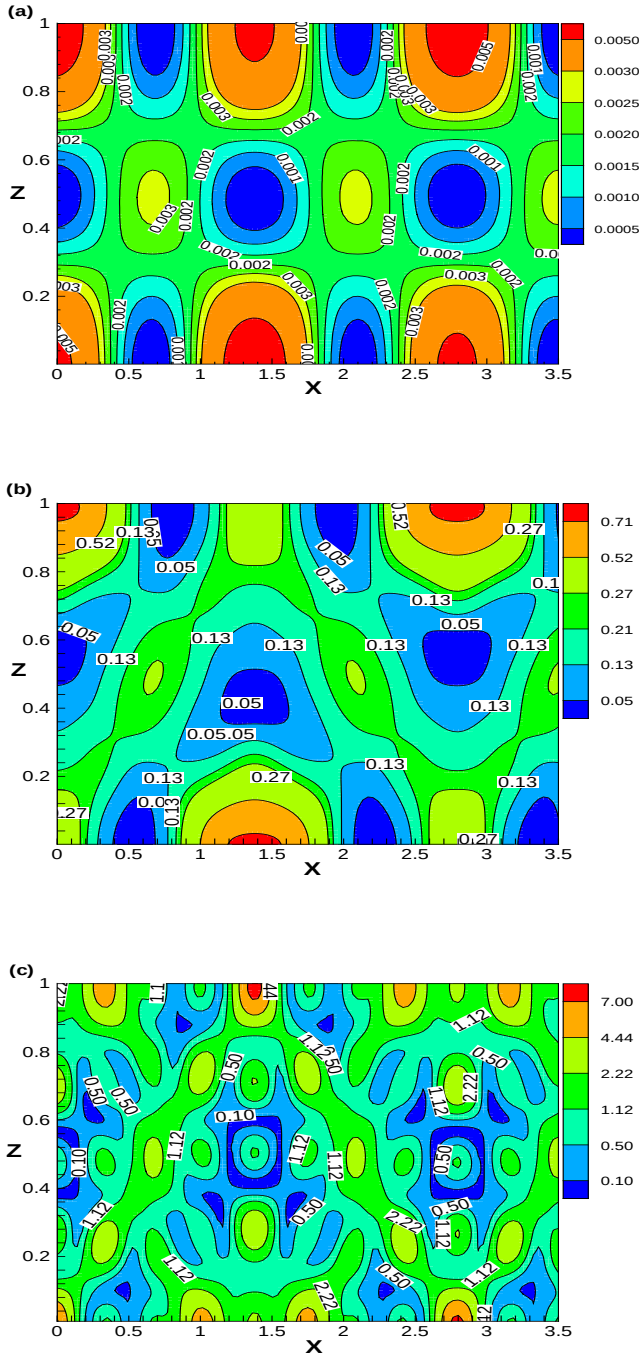

Fig. 2. Total entropy generation maps due to heat transfer and fluid friction for irreversibility distribution ratio $\varphi = 10^{-4}$ $Pr_1 = 0.025$ and $Q = 0$, (a) $Ra = 1.001 \times Ra_c$ (b) $Ra = 1.1 \times Ra_c$ (c) $Ra = 1.3 \times Ra_c$

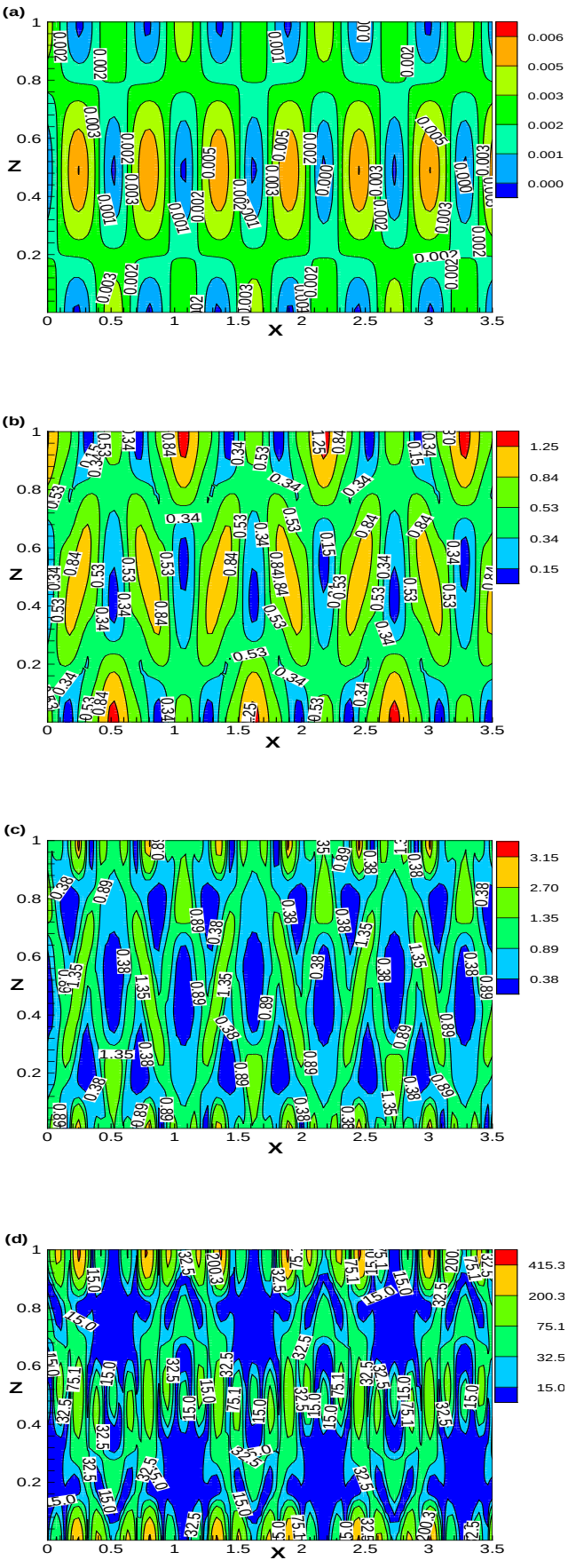

Fig. 3. Total entropy generation maps due to heat transfer and fluid friction for irreversibility distribution ratio $\varphi = 10^{-4}$ $Pr_1 = 0.025$, $Q = 1000$ and $Pr_2 = 0.001$, (a) $Ra = 1.001 \times Ra_c$ (b) $Ra = 1.3 \times Ra_c$ (c) $Ra = 1.6 \times Ra_c$ (d) $Ra = 3 \times Ra_c$

A further reorganization of entropy maps, due to enhanced thermal buoyancy, $Ra = 3 \times Ra_o$ is shown in Fig. 3(d). The maximum value of S_{gen} is increased from 3.3225 to 456.115, resulting in rapid heat transfer. The enhanced frictional irreversibility due to high thermal buoyancy generates multiple small entropy maps in the middle region. These multiple small entropy maps represent the dominance of the thermal field over magnetic field energy distribution. It is deduced from figs. 3(a - d) that the kinetic energy is strengthened by enhancing the parameter Ra, which in turn increases the rate of heat transfer in the system. It is also evident that the increment in Ra increases the boundary layer thickness. It is observed from Fig. 3(a-d) that an increase in the Rayleigh number tends to enhance the heat transfer. This phenomenon happens only in the presence of a higher Buoyancy force.

The effect of the magnetic field on entropy maps is presented in Fig. 4. The entropy maps in Figs. 4(a-c) are plotted for different values of Q with $Ra = 2700$, $Pr_1 = 0.021$ and $Pr_2 = 0.001$. The dynamic viscosity of the fluid is increased by enhancing the applied magnetic field, which resulted in the decrease of yield stress. The presence of a magnetic field in an electrically conducting fluid creates a resistive force called Lorentz force. It resists fluid motion, and as a result, the velocity of the fluid reduces due to an increase in magnetic parameter Q. The significant effect of the magnetic field is an increase in energy loss of the convective system, which in turn reduces the entropy generation due to fluid friction. Figure 4(a) represents energy distribution in the system for $Q = 100$. The entropy maps are smooth closed loops in the middle region while the semi-closed loops are restricted near boundaries. This represents the net influence of magnetic susceptibility ($Q = 100$) which is balanced by thermal buoyancy ($Ra = 2700$) on the fluid flow in the system. The local maximum and minimum values of S_{gen} are 0.0911 and 0.0003, respectively. The viscous force is comparable with the Lorentz force and the rate of heat transfer across the system stabilizes. Therefore the total entropy generation is low. The reason for the almost horizontal profile of the total entropy values is that the convection process transforms to conduction. This is due to the decline in kinetic energy when the high-intensity magnetic field is enhanced. So, the internal viscous and thermal waves are eliminated by Lorentz force. The total entropy generation map for $Q = 50$ is depicted in Fig. 4(b). As magnetic susceptibility is reduced, the thermal buoyancy dominates the energy distribution of the fluid flow across the system, the reorganization in total entropy maps is observed as shown in Fig. 4(b). The maximum value of S_{gen} is increased from 0.0911 to 300.328, as the applied magnetic field diminishes. It is interesting to observe that entropy maps with low energy values almost disappeared across both boundaries, as the magnetic field reduced from $Q = 100$(Fig. 4(a)) to $Q = 50$(Fig 4(b)). It can also be observed that multiple small local entropy maps are generated in the middle region, and entropy maps near boundaries extend up to the middle region due to dominant viscous force compared to the Lorentz force.

In Fig. 4(c), the total entropy maps are presented for

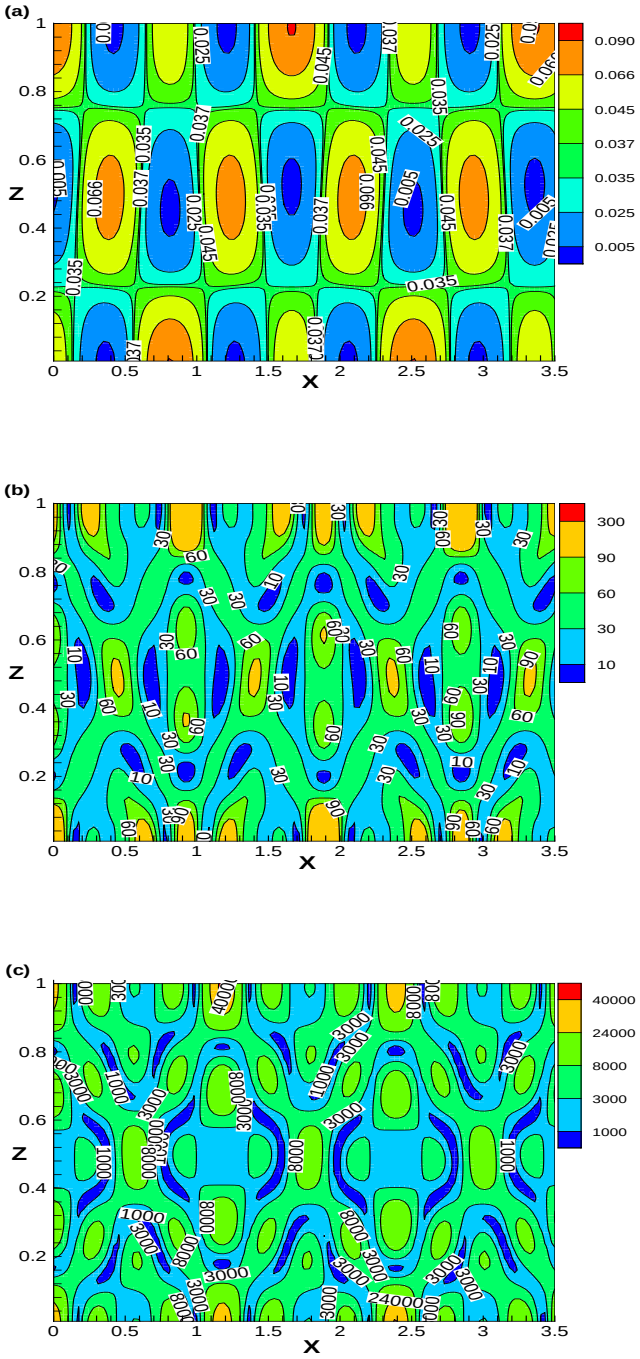

Fig. 4. Total entropy generation maps due to heat transfer and fluid friction for irreversibility distribution ratio $\varphi = 10^{-4}$, $Pr_1 = 0.021$, $Ra = 2700$, $Pr_2 = 0.001$, (a) $Q = 100$ (b) $Q = 50$ (c) $Q = 10$

$Q = 10$. The buoyancy force becomes dominant over the Lorentz force by decreasing Q. As a result, the heat transfer occurs rapidly. This phenomenon is observed from entropy maps depicted in Fig. 4(c). It is observed that the maximum value of S_{gen} is increased from 300.328 to 4195.3, as the applied magnetic field drops from $Q = 50$(Fig. 4(b)) to $Q = 10$(Fig. 4(c)). The entropy map distribution shows that with the enhancement of thermal buoyancy, the existence of high-temperature gradient and also due to the high-velocity level that causes stronger fluid friction. This is can be explained by the increase of velocity flow magnitude

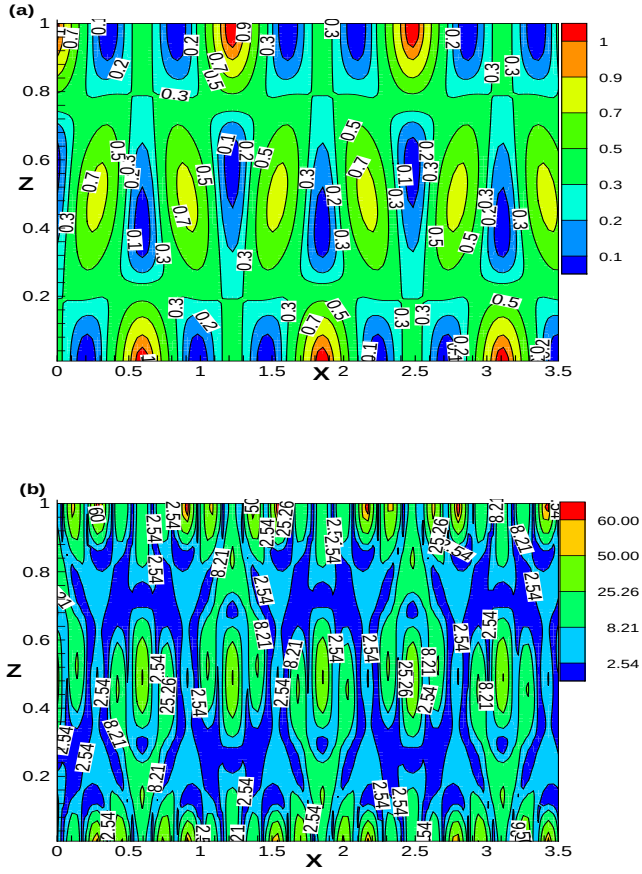

Fig. 5. Total entropy generation maps due to heat transfer and fluid friction for irreversibility distribution ratio $\varphi = 10^{-4}$, $Ra = 1.2 \times Ra_o$, $Q = 500$, $Pr_2 = 0.001$, (a) $Pr_1 = 0.025$ (b) $Pr_1 = 0.005$

caused by diminishing the magnetic field intensity. Thus as the Lorentz force decays, the more intermittent energy distribution is observed across the system.

Figure 5 illustrates the effect of thermal Prandtl number, Pr_1 on total entropy generation with the fixed values of $Ra = 1.2 \times Ra_o$, $Q = 500$ and $Pr_2 = 0.001$. The entropy maps for $Pr_1 = 0.025$ are depicted in Fig. 5(a). Entropy maps for total entropy generation that are uniformly distributed across the system represent the dominance of the conductive mode of heat transfer. The maximum and minimum values of S_{gen} are 1.0678 and 0.0208, respectively. The convective mode of energy distribution is observed as the value of Pr_1 is decreased from 0.025 to 0.005, as shown in Fig. 5(b). Upon decreasing the value of Pr_1, to 0.005, the entropy maps show highly intermittent energy distribution, as shown in Fig. 5(b). The maximum value of S_{gen} is increased from 1.0678 to 66.8127 as the value of Pr_2 decreased from 0.025 to 0.005. Multiple small local entropy maps are generated near both lower and upper boundaries and centrally located entropy maps extend up to boundaries due to an increase in thermal diffusivity over kinematic viscosity. The thermal diffusivity and kinematic viscosity differ in opposite directions, as Pr_1 variates. Thus the rise in the Pr_1 stabilizes the convection and the energy distribution across the system also gets stabilized, as similar

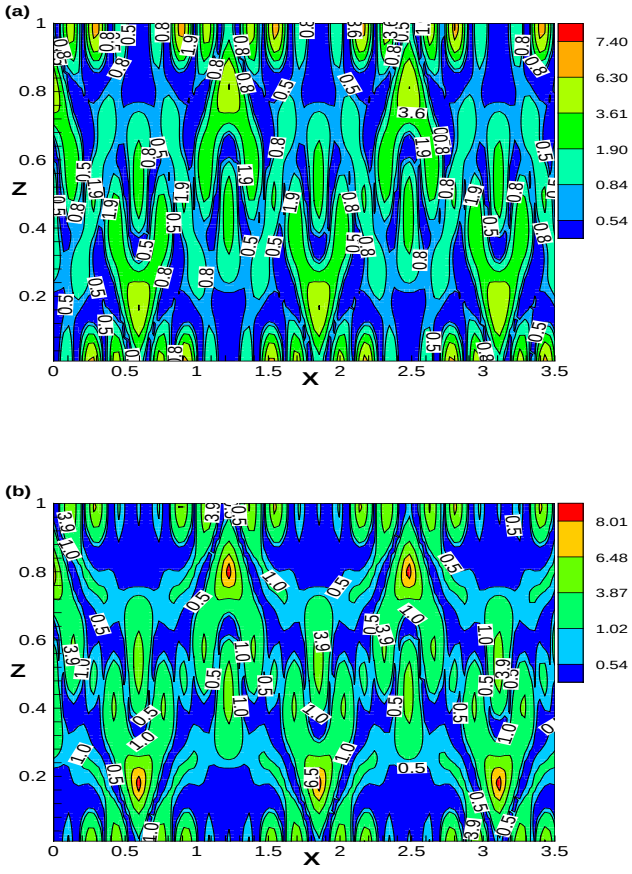

Fig. 6. Total entropy generation maps due to heat transfer and fluid friction for irreversibility distribution ratio $\varphi = 10^{-4}$, $Ra = 2 \times Ra_o$, $Q = 500$, $Pr_1 = 0.025$, (a) $Pr_2 = 0.001$ (b) $Pr_2 = 0.02$

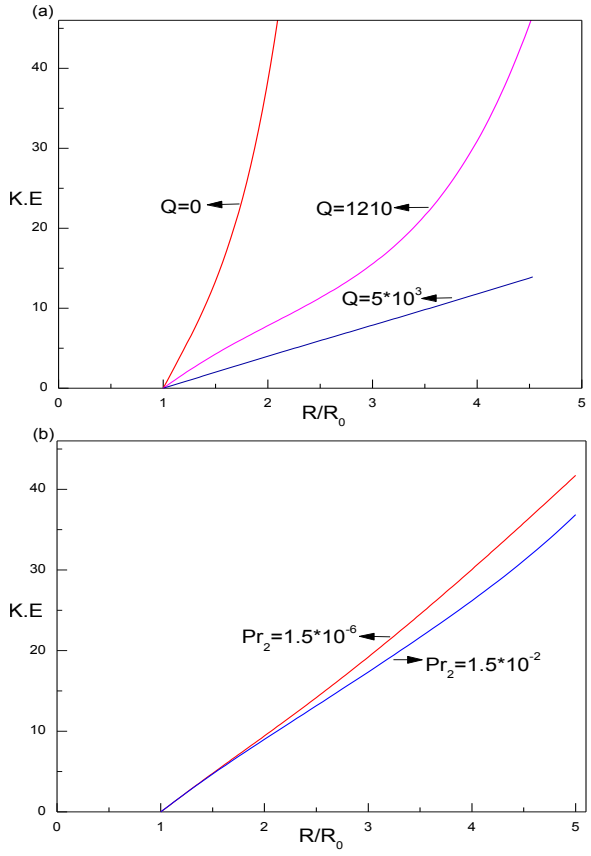

Fig. 7. Variation of kinetic with respect to R/R_0 for $Pr_1 = 0.025$ and $Pr_2 = 0.15 \times 10^{-6}$ (a) for different values of Q, (b) for different values of Pr_2

to Q.

The effect of Pr_2 on energy distribution is studied from total entropy generation maps depicted in Fig. 6, for $Ra = 2 \times Ra_o$, $Q = 500$ and $Pr_1 = 0.025$. Figure 6(a) is plotted for $Pr_2 = 0.001$ and the corresponding maximum and minimum values of S_{gen} are 7.4915 and 0.00905, respectively. The high-energy entropy maps are visible very close to boundaries. In Fig. 7(b), for $Pr_2 = 0.02$, the maximum and minimum values of S_{gen} are 8.4393 and 0.0179, respectively. As Pr_2 is incremented the maximum value of entropy also increases. The entropy maps of high energy values are visible close to boundaries as well as in the middle region. Upon increasing the value of Pr_2, the energy distribution in the system enhances. This is due to the attenuation of magnetic diffusivity and increase in thermal diffusivity. Thus convective system destabilizes as Pr_2 increases, which is similar to Ra.

The effect of applied vertical magnetic field on the kinetic energy of the fluid flow is presented in Fig. 7(a) for the values of $Pr_1 = 0.025$ and $Pr_2 = 0.15 \times 10^{-6}$ [15]. The variation of kinetic energy with respect to R/R_0 is studied for the values of $Q = 0$, $Q = 1210$ and $Q = 5 \times 10^3$ [16]. At a constant R, amplifying Q always causes a decrease in the kinetic energy. Thus, it can be stated that a vertical magnetic field has a damping effect on the kinetic energy of the system. The corresponding power law equations for $Q = 0$, $Q = 1210$ and $Q = 5 \times 10^3$ are $K.E = 0.993(R/R_0)^{4.964}$, $K.E = 0.781(R/R_0)^{3.006}$ and $K.E = 1.232(R/R_0)^{2.419}$, respectively. It can be noted that by increasing Q values, the power law of the exponent decreases as well. In the absence of the magnetic field ($Q = 0$), the power law exponent of kinetic energy is 5 times with respect to normalised temperature (R/R_0). In comparison with nonmagnetic field ($Q = 0$), the kinetic energy is reduced approximately to three fold i.e., the power law exponent is 3.006 for $Q = 1210$. Considering the fact of suppression of velocity fluctuations by an imposed magnetic field, one would expect a reduction of the kinetic energy of the fluid. The results of kinetic energy are in accordance with the results of entropy generated in the system. Similarly, the effect of magnetic Prandtl number on kinetic energy is presented in Fig. 7(b). The variation of kinetic energy with respect to R/R_0 is analyzed for $Pr_2 = 1.5 \times 10^{-6}$ and $Pr_2 = 1.5 \times 10^{-2}$. The corresponding power law equations for $Pr_2 = 1.5 \times 10^{-6}$ and $Pr_2 = 1.5 \times 10^{-2}$ are $K.E = 1.063(R/R_0)^{2.511}$ and $K.E = 0.730(R/R_0)^{2.730}$, respectively. The kinetic energy shows a damping effect with an increase in Pr_2, for a given value of R. Similar to the vertical magnetic field, the magnetic Prandtl number also stabilizes the convective system and hence heat transfer diminishes.

V. Conclusion

The problem of energy distribution in laminar natural convection under an externally applied vertical magnetic field is evaluated numerically by using the entropy generation principle. Entropy generation rates play an important role in the overall thermal mixing of fluid within the cavity. The effect of Chandrasekhar number Q, thermal (Pr_1), and magnetic (Pr_2) Prandtl numbers on total entropy generation is considered simultaneously. Entropy generation due to a magnetic effect, fluid friction as well as heat and mass transfer has been evaluated for laminar flow in the transient state for stress-free boundary conditions. The total entropy enhances as thermal buoyancy generated increases due to a higher degree of irreversibility associated with heat transfer and fluid flow. It is well known that under the influence of an externally applied vertical magnetic field, the convective currents are diminished. It is observed that under uniform thermal buoyancy the total entropy generated enhances with a decrease of the magnetic field. As Pr_2 gets incremented, the total entropy generation in the fluid across the layer increases, and the flow is accentuated as Pr_1 increases. It is also shown that the kinetic energy of the fluid is reduced by the application of a vertical magnetic field, thereby reducing the velocity fluctuation. The results of entropy generated in the system and kinetic energy of the fluid flow are in reasonable agreement with the results of Rameshwar et al. [13].

References

[1] Grossmann, S. and Lohse, D. *Phys. Rev. E*, 66 016305, 2002.

[2] Ahlers, G. Grossmann, S. and Lohse, *D. Rev. Mod. Phys.*, vol. 81, pp. 503537, 2009.

[3] Frick, P. Khalilov, R. Kolesnichenko, I. Mamykin, A. Pakholkov, V. Pavlinov, A. and Rogozhkin, *S. Europhys. Lett.*, vol. 109, 14002, 2015.

[4] F. Salah, Z.A. Aziz, DLC. Ching, On accelerated MHD flows of second grade fluid in a porous medium and rotating frame *IAENG International Journal of Applied Mathematics*, vol. 43 Issue 3, pp. 106-113, 2013.

[5] D.Y. Shagaiya, Z.A. Aziz, I. Zuhaila, F. Salah, Slip Effects on Electrical Unsteady MHD Natural Convection Flow of Nanofluid over a Permeable Shrinking Sheet with Thermal Radiation, *Engineering Letters*, Vol. 26 Issue 1, pp. 107-116, 2018.

[6] O.A. Saunders, Natural Convection in Liquids, *Proc. Roy. Soc. (London)*, Ser. A, vol. 172, pp. 55-71, 1939.

[7] M. Fumizawa, Natural convection experiment with liquid NaK under transverse magnetic field, *J. Nucl. Sci. Tech.*, vol. 17, 98105, 1980.

[8] A.El. Jery, N. Hidouri, M. Magherbi, and A. Ben Brahim, Effect of an External Oriented Magnetic Field on Entropy Generation in Natural Convection, *Entropy*, Vol. 12, No.6, pp.1391-1417, 2010.

[9] A. Bejan, Entropy generation minimization, *CRC Press. Boca Raton*, 1966.

[10] A. Bejan, Second-law analysis in heat transfer and thermal design, *Adv. Heat Transf*, vol. 15, pp. 158, 1982.

[11] S. Saravanan, P. Kandaswamy, Low Prandtl number magnoconvection in cavities: Effect of variable thermal conductivity, *Z. Angew. Math. Mech.*, vol. 80, pp. 570576, 2000.

[12] H.L. Kuo, Solution of the non-linear equations of the cellular convection and heat transport, *J. Fluid Mech.*, vol. 10, pp. 611-630, 1961.

[13] Y. Rameshwar, M.A. Rawoof Sayeed, H.P. Rani, D. Laroze, Finite amplitude cellular convection under the influence of a vertical magnetic field, *Int. J. Heat and Mass Transfer*, vol. 114, pp. 559-577, 2017.

[14] S. Chandrasekhar, Hydrodynamic and Hydromagnetic Stability, *Oxford University Press*, 1961.

[15] H.L. Kuo, Power laws of high Rayleigh number convection, *Boundary layer Meterology*, vol. 17, pp. 29-39, 1979.

[16] J. M. Aurnou, P. L. Olson, Experiments on Rayleigh-Benard convection, magnetoconvection and rotating magnetoconvection in liquid gallium, *J. Fluid Mech.*, vol. 430, pp. 283-307, 2001.